Multidimensional Modeling of Fuel Composition Effects on Combustion and Cold-starting in Diesel Engines

Nabil S. Ayoub, and Rolf D. Reitz

University of Wisconsin-Madison

ABSTRACT

A computer model developed for describing multicomponent fuel vaporization, and ignition in diesel engines has been applied in this study to understand cold-starting and the parameters that are of significant influence on this phenomena. This research utilizes recent improvements in spray vaporization and combustion models that have been implemented in the KIVA-II CFD code. Typical engine fuels are blends of various fuels species, i.e., multicomponent. Thus, the original single component fuel vaporization model in KIVA-II was replaced by a multicomponent fuel vaporization model (based on the model suggested by Jin and Borman). The model has been extended to model diesel sprays under typical diesel conditions, including the effect of fuel cetane number variation. Necessary modifications were carried out in the atomization and collision sub-models. The ignition model was also modified to account for fuel composition effects by modifying the Shell ignition model. The improved model was applied to simulate diesel engine cold-starting. The effect of fuel residual from previous cycles was studied and was found to be important. Other injection parameters, such as injection timing and duration were also studied. Another factor that was investigated was engine geometry and how it can be modified to improve on cold-starting in diesel engines. Cold-starting was found to be enhanced by the presence of a small fuel vapor residual and by a shorter injection duration, while engine geometry modifications were found to be helpful in selecting an optimum location on the cylinder head for an ignition aid.

THE SIGNIFICANT NUMBER of diesel engines which provide automotive power, together with recent concerns for the environment, resulted in the introduction of more legislation to limit their pollutant emissions. Of particular interest are the Nitrogen Oxides (NOx) and soot emissions. Both of these pollutants depend significantly on both the fuel and the injection system. The trend to lower emissions motivates new research efforts with the objective of improving engine performance. A significant fraction of engine emissions, particularly unburned hydrocarbons, is produced during the cold-starting phase of the engine operation.

Furthermore, starting the diesel engine under cold ambient conditions represents a difficulty in itself Thus, more research is needed to identify mechanisms that would improve the cold-startability of the engine. Cold-starting is characterized as a situation where the engine does not fire at all for several cycles, or fires for one cycle and skips firing for the several following cycles, as seen by Henein et al. [1]*. There are several other issues of importance in cold-starting of diesel engines as discussed in Gonzalez et al. [2]. Fuel carryover from cycle-to-cycle is important as liquid fuel remains on the piston surface from misfiring and borderline cycles. Also, another factor in cold-starting in diesels is the excessive wear that results from high peak pressures reached after combustion after misfiring. Blowby gases also tend to increase at the slower cranking speed and that further reduces the compression temperature. Finally, the issue of unburned hydrocarbons and white smoke contributes significantly to the engine emissions. The objective of this work is to understand the process of cold-starting and the various parameters that can help improve the cold-startability of the engine using the most updated and improved computational models in KIVA-II.

The controlling processes in diesel engine combustion are very complicated. To have a better understanding of these processes, they can be broken down to several distinct sub-processes such as injection, atomization, vaporization, ignition, combustion, etc. Once each process is investigated, a comprehensive understanding of diesel combustion can be achieved.

---

* Numbers in brackets designate references listed at the end of the paper.

Report Documentation Page

Form Approved
OMB No. 0704-0188

1. REPORT DATE	2. REPORT TYPE	3. DATES COVERED
JAN 1995		**00-00-1995 to 00-00-1995**

4. TITLE AND SUBTITLE	5a. CONTRACT NUMBER
Multidimensional Modeling of Fuel Composition Effects on Combustion and Cold-starting in Diesel Engines	5b. GRANT NUMBER
	5c. PROGRAM ELEMENT NUMBER
6. AUTHOR(S)	5d. PROJECT NUMBER
	5e. TASK NUMBER
	5f. WORK UNIT NUMBER
7. PERFORMING ORGANIZATION NAME(S) AND ADDRESS(ES) **University of Wisconsin-Madison ,716 Langdon St,Madison,WI,53706-1481**	8. PERFORMING ORGANIZATION REPORT NUMBER
9. SPONSORING/MONITORING AGENCY NAME(S) AND ADDRESS(ES)	10. SPONSOR/MONITOR'S ACRONYM(S)
	11. SPONSOR/MONITOR'S REPORT NUMBER(S)

12. DISTRIBUTION/AVAILABILITY STATEMENT
Approved for public release; distribution unlimited

13. SUPPLEMENTARY NOTES

14. ABSTRACT

A computer model developed for describing multicomponent fuel vaporization, and ignition in diesel engines has been applied in this study to understand cold-starting and the parameters that are of significant influence on this phenomena. This research utilizes recent improvements in spray vaporization and combustion models that have been implemented in the KIVA-II CFD code. Typical engine fuels are blends of various fuels species, i.e., multicomponent. Thus, the original single component fuel vaporization model in KIVA-II was replaced by a multicomponent fuel vaporization model (based on the model suggested by Jin and Borman). The model has been extended to model diesel sprays under typical diesel conditions, including the effect of fuel cetane number variation. Necessary modifications were carried out in the atomization and collision sub-models. The ignition model was also modified to account for fuel composition effects by modifying the Shell ignition model. The improved model was applied to simulate diesel engine cold-starting. The effect of fuel residual from previous cycles was studied and was found to be important. Other injection parameters, such as injection timing and duration were also studied. Another factor that was investigated was engine geometry and how it can be modified to improve on cold-starting in diesel engines. Cold-starting was found to be enhanced by the presence of a small fuel vapor residual and by a shorter injection duration, while engine geometry modifications were found to be helpful in selecting an optimum location on the cylinder head for an ignition aid.

15. SUBJECT TERMS

16. SECURITY CLASSIFICATION OF:			17. LIMITATION OF ABSTRACT	18. NUMBER OF PAGES	19a. NAME OF RESPONSIBLE PERSON
a. REPORT **unclassified**	b. ABSTRACT **unclassified**	c. THIS PAGE **unclassified**	**Same as Report (SAR)**	**11**	

For combustion to start in a fuel spray, the droplets must vaporize partially. Thus, the ignition delay (the delay between the start of injection and the start of combustion), as well as the rate of combustion are strong functions of the droplet vaporization rate [3]. Consequently, the overall engine combustion process and as a result, its efficiency, emissions and cold-starting performance are directly affected by the vaporization process as shown in Ayoub and Reitz [4]. Predicting droplet vaporization accurately would lead to better prediction of the overall combustion process, including both the emissions and starting.

Recently a detailed multidimensional code for modeling reactive flows, such as those encountered in internal combustion engines, has been developed. This code, KIVA-II, includes a model for spray dynamics, a statistical representation that accounts for a spectrum of droplet sizes and the effects of evaporation on sprays, as well as droplet breakup, collision, and coalescence [5]. Spray computations show the sensitivity of the results to the droplet life-time that is, in turn, dependent on the vaporization process. The vaporization models have been extensively discussed by Ayoub and Reitz [4] and results were presented for single droplets with comparison to experimental data, for sprays and several engine cases. The present study utilizes the model improvements that were presented by Ayoub and Reitz [4] in addition to improvements to the ignition model. The goal of this study is to apply the improved models that will be discussed in the next section, to study the sensitivity of diesel combustion to fuel composition as well as investigating factors that are important in cold-starting of diesel engines.

MODEL FORMULATION

The KIVA-II code [5] was used in this study with improvements in the spray, ignition, combustion, and emission models. The code solves the mass, momentum and energy conservation equations, coupled with the k-ε turbulence model in three dimensions as a function of time. The interactions between the spray droplets and the gas phase are also accounted for. Since the governing equations in the KIVA-II code are documented in Ref. [5], only the improved submodels will be discussed. Other improvements in the wall heat transfer and spray-wall impingement models that were also incorporated in the present study have already been discussed by Kong and Reitz [6], Reitz [7] and Gonzalez et al. [2]. Flow through the ring crevice was accounted for using a phenomenological crevice flow model [7, 8] that was coupled to the KIVA solution.

Fuel Vaporization Model - The fuel droplets exiting the spray nozzle undergo a process of "heat-up" and internal mixing due to the relatively high relative velocities they are subjected to. To account for this phenomena of internal mixing, the finite conduction model with adjusted or "effective" transport parameters was used as in Jin and Borman [9].

This model is a comprehensive model that handles high-pressure effects in multicomponent fuel vaporization. The basic assumptions in this model are : droplets are spherically symmetric, pressure is uniform in space around the droplet, gas-liquid interface is in thermodynamic equilibrium, no cross effects exist between heat and mass transfer, and gas is dissolved in a very thin liquid surface layer (i.e., gas does not diffuse into the interior).

This model does not only account for high pressure effects, but also it takes into consideration the following non-ideal phenomena: variable gas and liquid properties, non-ideal gas effects at the droplet interface, high mass transfer corrections on heat and mass transfer, heat and mass diffusion inside the droplet, and internal mixing effects.

Gas and liquid properties are evaluated as a function of temperature since this is the main parameter that accounts for the property variations. Such properties include density, specific heat, viscosity, and mass diffusivity. However, in the case of density, pressure effects are equally important for both the gas and liquid phase. For the gas phase, a modified Redlich-Kwong equation of state is used (Prausnitz, [10]). In the liquid phase, the partial molar volumes of the individual components (Reid et al., [11]) are used along with the liquid composition to account for the effect of pressure on the density.

In previous experiments and studies (El-Wakil et al., [12] and Abramazon and Sirignano, [13]), it was found that problems that involve high mass transfer rates should include some corrections in the heat and mass transfer coefficients. The presence of such high mass transfer rates tend to further slow down heat and mass transfer processes due to the accumulation of vapor around the droplets. The corrections are included in the present model.

In the liquid phase, the Jin & Borman model predicts the transient behavior of the droplet by solving the heat and mass diffusion equations numerically rather than using a lumped parameter solution, which gives unsatisfactory results due to the presence of significant heat and species gradients inside the droplet.

The governing equations for the gas and liquid models are described in detail in Jin and Borman [9]. The most fundamental equation that is used in this model is the phase equilibrium relationship for all the components in both phases as shown by equation (1) :

$$f_i^l = f_i^v \qquad \text{for} \qquad i = 1,\ldots,n \qquad (1)$$

i.e., the fugacity of each fuel component is the same in both the liquid and the vapor phases. Fugacity is an indication of the equilibrium pressure, and takes into account all the liquid and vapor non-idealities due to high pressure. The rest of the model is described in detail in Prausnitz and Chuen [14].

Ignition Modeling - The low-temperature chemistry of hydrocarbon fuels must be described to be able to predict the ignition delay in diesel engines accurately. In this study, the Shell model (Halstead et al., [15]) was used for ignition kinetics modeling. The model uses a reduced kinetic mechanism which contains five generic species and eight generic reactions to simulate the autoignition phenomena of hydrocarbon fuels. Details of the ignition model are discussed in Halstead et al. [15], Kong and Reitz [16], and Kong et al. [17].

Since the study considers several species of fuel, special attention has to be given to the ignition of a mixture of different species. The Shell ignition model assumes a generic fuel species of the chemical formula C_nH_{2m}, and the fuels of interest in this investigation are of similar chemical formula. The ignition characteristics of a diesel fuel are assumed to be given by the local Cetane number (CN) of that fuel at each point in the combustion chamber. The higher the CN, the more readily the fuel ignites, and vice versa. The local composition of the fuel in the engine determines the CN which is used to determine the ignition rate. There have been several suggestions in the literature to account for the effect of CN on ignition rates such as those by Ramos [18] and by Heywood [19]. Heywood suggested a correlation in which the ignition activation energy is adjusted for CN changes using:

$$E_A = \frac{618840}{CN + 25} \qquad (2)$$

The simplified reaction mechanism used in the Shell model consists of eight generic reactions based on the degenerate branching characteristics are formulated from five generic species. The reactions and species involved in this kinetic model are as follows:

$RH + O_2 \rightarrow$	$2R^*$	K_q	(3a)
$R^* \rightarrow$	$R^* + P + \text{Heat}$	K_p	(3b)
$R^* \rightarrow$	$R^* + B$	f_1K_p	(3c)
$R^* \rightarrow$	$R^* + Q$	f_4K_p	(3d)
$R^* + Q \rightarrow$	$R^* + B$	f_2K_p	(3e)
$B \rightarrow$	$2R^*$	K_b	(3f)
$R^* \rightarrow$	termination	f_3K_p	(3g)
$2R^* \rightarrow$	termination	K_t	(3h)

where RH is the hydrocarbon fuel (C_nH_{2m}), R^* is the radical formed from the fuel, B is the branching agent, Q is a labile intermediate species, and P is oxidized products, consisting of CO, CO_2, and H_2O in specified proportions. The expressions for K_q, K_p, K_b, K_t, f_1, f_2, f_3, f_4 etc. are those given by Halstead et al. [15].

Of the eight reactions shown above, reaction (3d) was shown in Kong and Reitz [16] to be a crucial path for the intermediate ignition species, Q, to transform into branching species, B. Thus the proposed Cetane Number modification was included in evaluating the rate of reaction of reaction (3d). Thus the activation energy of the reaction, E_{f4}, was modified by the following correction:

$$E^*_{f4} = E_{f4}\frac{65}{CN + 25} \qquad (4)$$

In other words, for a CN of 40, which is a very typical CN for diesel fuels, the correlation factor is 1, and for higher values of CN, the activation energy decreases resulting in shorter ignition delays and vice versa.

The cetane number is evaluated directly as a function of fuel composition. By using a blend of cetane (hexadecane) which has a cetane number of 100, and iso-cetane (α-methyl-naphthalene) which has a cetane number of 0, it is possible to achieve blends with a wide range of cetane numbers. Moreover, the cetane numbers used in the ignition model are the local values of cetane number within the engine since the two components could be vaporizing at different rates due to their volatility differentials.

Combustion - In diesel engines, a significant portion of combustion is thought to be mixing-controlled. Hence, interactions between turbulence and chemical reactions have to be considered. A laminar-and-turbulent characteristic-time combustion model was used for the present study. The local time rate of change of the partial density of species m, due to conversion from one chemical species to another, is given by

$$\frac{dY_m}{dt} = -\frac{Y_m - Y^*_m}{\tau_c} \qquad (5)$$

where Y_m is the mass fraction of species m, Y^*_m is the local and instantaneous thermodynamic equilibrium value of the mass fraction, and τ_c is the characteristic time for the achievement of equilibrium. To predict thermodynamic equilibrium temperatures accurately, it is sufficient to consider seven species: fuel, O_2, N_2, CO_2, CO, H_2, and H_2O, and to assume that the characteristic time τ_c is the same for all seven. As was previously assumed for the ignition model, the two fuel species are combined into an "effective" fuel for the purposes of the present implementation of the combustion model.

The model was combined with the ignition model to simulate the overall combustion process as described by Kong and Reitz [16]. The ignition model was used whenever and wherever the temperature was lower than 1000 K to simulate the ignition chemistry and locate the ignition cells. If the temperature was higher than 1000 K, the combustion model was activated for describing high temperature chemistry.

The characteristic time τ_c is the sum of a laminar timescale and a turbulent timescale,

$$\tau_c = \tau_l + f\tau_t \qquad (6)$$

The laminar timescale τ_l is derived from an Arrhenius-type reaction rate (Bergeron and Hallett, [20]) with the pre-exponential constant $A=7.68\times10^8$ and the activation energy E=77.3 kJ/mol :

$$\tau_l = A^{-1}[\text{fuel}]^{0.75}[O_2]^{-1.5}\exp\left(\frac{E}{RT}\right) \qquad (7)$$

The turbulent timescale τ_t is proportional to the eddy turnover time,

$$\tau_t = C_2\frac{k}{\varepsilon} \qquad (8)$$

where C_2=0.1 (Kong et al., [21]), and k and ε are calculated from the modified RNG k-ε turbulence model [17]. The delay coefficient (given by $f = (1 - e^{-r})/0.632$,) simulates the increasing influence of turbulence on combustion after ignition has occurred, and *r* is the ratio of the mass of products to that of total reactive species. The parameter *r* indicates the completeness of combustion in a specific region. Its value varies from 0 (no combustion yet) to 1 (complete consumption of fuel and oxygen). Accordingly, the delay coefficient *f* changes depending on local conditions. This approach is conceptually consistent with the mixing combustion model of Magnussen et al. [22]. The above combustion model has been found to give accurate results [21].

RESULTS

The improved multicomponent vaporization model was successfully implemented in KIVA-II and applied to vaporizing sprays under diesel engine conditions (Ayoub and Reitz [23]). Results from these studies showed the importance of ambient temperature in multicomponent fuel vaporization particularly at cold-starting conditions. Of importance also was droplet breakup and size distribution with larger droplets being more controlled by diffusion inside the droplets.

Warm Engine Computations - Having implemented the multicomponent fuel vaporization model in KIVA-II for single droplets and then for sprays, the next step was to apply it to a diesel engine computation using all the improved models that were added previously to KIVA-II [24]. Experimental results from a single cylinder version of the Caterpillar 3406 diesel engine were used in this study for comparison with the model calculations for the standard "warm" engine operating condition case. The engine has been well characterized in previous experimental and computational studies, including emissions measurements (Nehmer, [25]; Tow et al., [26]), in-cylinder gas temperature (Giangregorio et al., [27]), gas velocity measurements (Sweetland et al., [28]), and realistic intake flow computations (Rutland et al., [29]). Details of the engine specifications are given in Table 1.

Table 1 Caterpillar Engine Specifications and Standard "warm" Operating Conditions

Bore	137.19 mm
Stroke	165.1 mm
Connecting Rod Length	261.62 mm
Displacement	2.44 L
Compression Ratio	15.0
Piston crown	Mexican hat
Engine Speed	1600 rpm
Intake pressure	184 kPa
Intake temperature	310 K
Fuel Injected	0.1622 g/cycle
Intake valve close timing	147 deg. BTDC
Swirl ratio (nominal)	1.0

The computations in this study considered single injections with an injection pressure of 90 MPa, with a start of injection timing of -11° CA atdc. The nozzle tip had six holes with hole diameters of 0.259 mm and an included angle between fuel sprays of 125 degrees. This results in significant spray impingement on the piston. The injection featured fast opening and closing rates (~2 crank angle degrees for opening and closing--Nehmer et al., [30]) and the experimental injected mass flow rates were used to compute the injection velocities for the computations.

Cylinder pressures, needle lifts and rate of injection profiles (obtained using a Bosch rate-of injection meter) were monitored in the experiments. The experimental injection profile was used for both normal and cold-starting conditions. The experimental pressure data were analyzed by a heat release analysis (Tree, [31]). More details about the experimental conditions are given in (Nehmer et al., [30]).

The computational mesh used represents one-sixth of the combustion chamber in the engine (i.e., a 60° sector) for computational efficiency, since it has six injector holes. Thus, the computational domain had periodic boundary conditions. There were 20 cells in the radial direction, 30 cells in the azimuthal direction and 18 cells in the axial direction with 5 cells in the squish region at top dead center. Previous results (Gonzalez et al., [32]) indicate that the computations are most sensitive to the grid resolution in the azimuthal direction, and the present resolution was found to give adequately grid-independent results (Patterson et al., [24]). Typical computer times were about 2-3 Cray-YMP hours for each run. The fuel used in the experiment was Amoco Premier #2 (Cetane Number of 40) which was modeled using a cetane/iso-cetane blend. The computation was performed for 3 blends with cetane numbers of 35, 40, and 45. The blend cetane number was determined by the percentage of iso-cetane in the fuel injected.

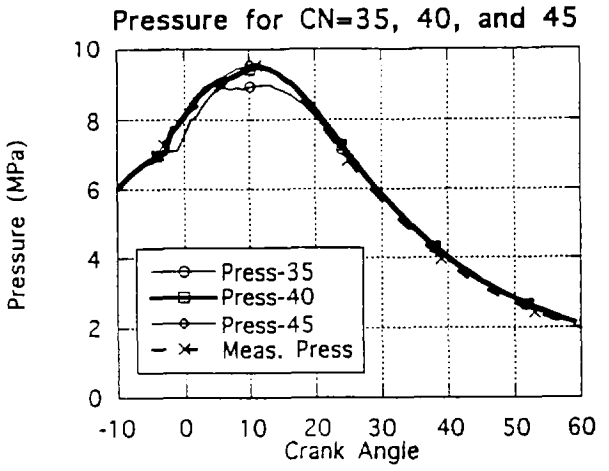

Figure 1 Engine pressure for CN = 35, 40, and 45 with experimental data for CN = 40.

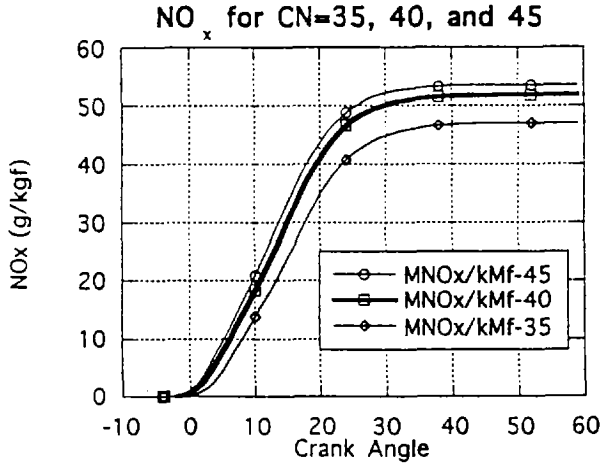

Figure 2 NOx mass produced per unit mass of injected fuel for the computed cases in Fig. 1.

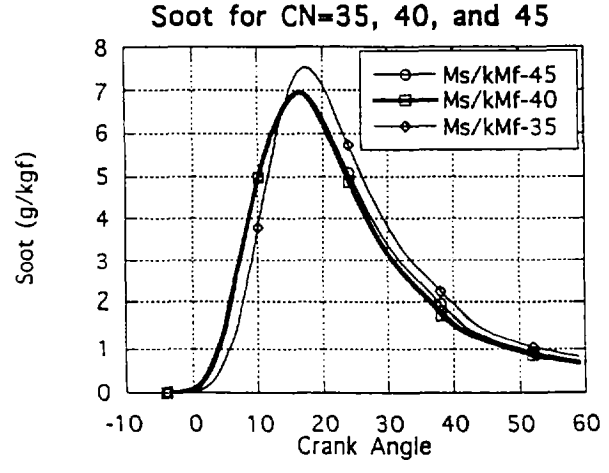

Figure 3 Soot mass produced per unit mass of injected fuel or the computed cases in Fig. 1.

The CN-40 fuel is considered the reference fuel that is representative of diesel fuels. Figure 1 shows the computed pressure for the three cases along with the experimental pressure trace. The CN-40 case agrees well with the experiment with ignition taking place at -3° CA. The CN-45 case is very similar to the CN-40 case but with ignition taking place slightly earlier at -4° CA. However, significant differences could be observed in the CN-35 case where ignition occurred at -0.5° CA which resulted in not reaching the peak experimental pressure. The trend in ignition delay was noticed when the cetane number is changed from 45 to 35 is consistent with the expected fuel performance.

Emissions results are shown in Figs. 2 and 3 for the three cases. While there is no clear trend in the soot engine-out results, there is a definite relationship between the NOx and CN. As shown in Fig. 2, the CN-45 had the most engine-out NOx due to the earlier ignition, while the CN-35 case had the least NOx due to the later ignition and lower peak temperatures. Thus NOx decreases with lower CN and that is consistent with experiments. In the case of soot, the CN-35 case produced the highest in-cylinder peak values of soot. This is explained by the fact that there was more vaporized fuel in the cylinder that was available for soot production (when compared to the other two cases) due to the fact that ignition in the CN-35 case was delayed. Temperature contours are shown for all 3 cases just at or after ignition in each case in Fig. 4. The CN-40 and the

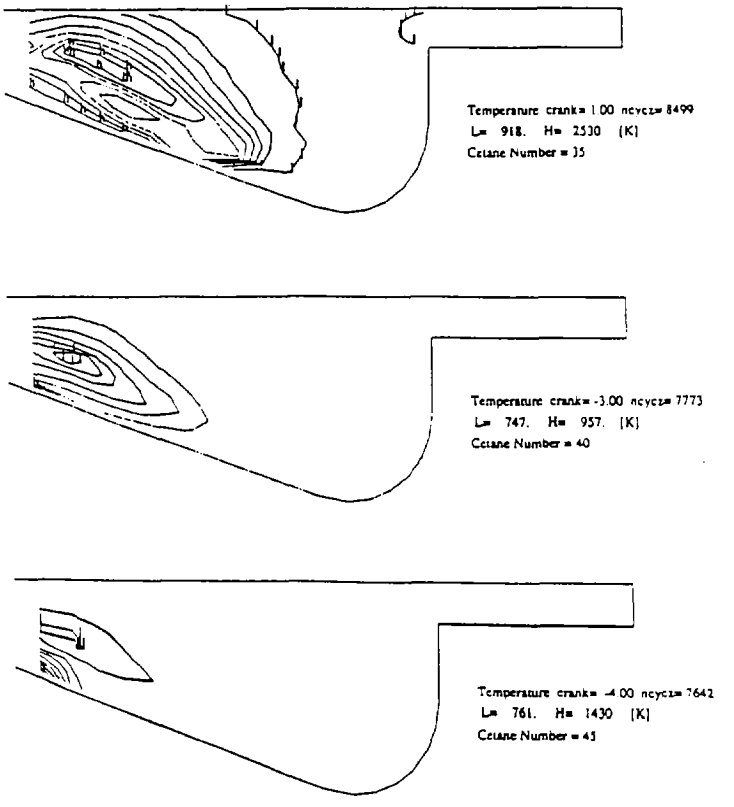

Figure 4 Temperature contours at or just after ignition for the computed cases in Fig. 1.

Table 2 Engine cases and ignition results

Case	Tair [K]	Injection	Residual	Rim	CA (T=1000 K)	CA (T=1500 K)	CA (T=2000 K)
1	273	10.75°	0% 1F	None	10.02	10.08	15.50
2	273	10.75°	10% 1F	None	5.750	6.640	> 6.64
3	273	21.50°	10% 1F	None	14.05	17.46	> 17.46
4	273	10.75°	5% 1F	None	6.850	7.230	8.230
5	254	10.75°	10% 1F	None	9.020	10.86	13.09
6	254	10.75°	10% 2F	None	-1.36	0.700	2.020
7	254	10.75°	10% 1F	Square	18.98	21.93	22.89
8	254	10.75°	10% 2F	Notched	-1.80	-1.27	2.590
9	254	10.75°	5% 2F	Notched	-0.77	7.260	8.150

CN-45 cases show very similar contours with ignition occurring just underneath the nozzle. In the CN-35 case, due to deeper spray penetration at the time of ignition, there was more fuel mixing and ignition occurred on either side of the spray.

Cold Engine Computations - The modified KIVA code was applied to the same engine described above but under cold-starting conditions. The cases that were considered for the purpose of this study are listed in Table 2. The results of these cases will be presented next with special emphasis on the fuel droplet and vapor distributions within the computational domain and their impact on ignition.

There are two fundamental differences in the operating conditions (other than the ambient temperature). The first difference is that the engine speed is significantly lower than that at warm engine conditions. For the purpose of this part of the study, the cranking engine speed is assumed to be variable. Experimental measurements during cold-starting (Poublon [33]) show reductions in the engine speed during the compression stroke as the piston approaches TDC. It is assumed for the purpose of this computation that the engine speed follows a sine wave profile with 100 rev/min as the average speed and with a 50 rev/min variation. Thus the instantaneous engine speed is given by:

$$rpm = 100 - 50 * \sin(CA + 90) \qquad (9)$$

The other difference is that the intake pressure is atmospheric pressure rather than the boost pressure. The rest of the parameters that were changed are listed in Table 2.

The cases listed above are primarily for two intake air temperatures, 273 K (cases 1-4) and 254 K (cases 5-9). In Ayoub and Reitz [4], lower intake air temperature cases (241 K) were investigated and ignition did not occur due to the long ignition delay. Thus for the purpose of this study, moderate cold air intake temperatures were considered.

Another parameter that was investigated was the injection duration. It was shown in Ayoub and Reitz [4], that advancing injection timing helps ignition under cold-starting conditions, since the fuel droplets do not atomize as they would under warm conditions and thus vaporization is constrained by diffusion. In this study the start of injection was maintained at -11° CA ATDC (the standard start of injection) but the duration of injection was halved to 10.75°, except for case 3 where the standard duration of injection was used. This was done in an attempt to increase droplet atomization by increasing the velocity of the droplets coming out of the injector nozzle.

Previous experiments such as those done by Henein and Zadeh [34] showed that the engine under cold-starting conditions may skip several cycles between firings with a defined frequency. This can be explained by the accumulation of residual fuel inside the cylinder from non-firing cycles until the amount of fuel reaches a certain level and this helps to fire the engine. Based on this observation, a factor that was considered in this study is introducing a homogeneously distributed fuel residual in the vapor phase at intake valve closure to help start ignition. As shown in Table 2, there are cases with no residual, and cases with 10% and 5% residuals. Among these cases the composition of the residual was changed from 100% iso-cetane (the cases denoted by 1F) to 40% iso-cetane/60% cetane (the cases denoted by 2F). This was important in the study to study the effects of fuel composition on ignition .

The final parameter that was changed is the engine geometry. The standard piston bowl was modified to a reentrant bowl by using a variety of rims. A square rim was tested in case 7 and then a notched rim was used in cases 8 and 9. In the following section the results of these cases will be presented and some guidelines for improving cold-startability will be suggested based on the predicted results.

The pressure results of these cases are displayed in Figs 5, 6, and 7. Although ignition started in case 1, combustion did not develop significantly as seen in Fig. 5. The effect of the 10% residual fuel is evident in cases 2 and 3, as the top dead center pressure is higher in these two cases due to the initial heat release from the residual fuel. In either case, ignition did not happen while the spray was being injected since the temperature resulting from the oxidation of the residual fuel was below 1000 K.

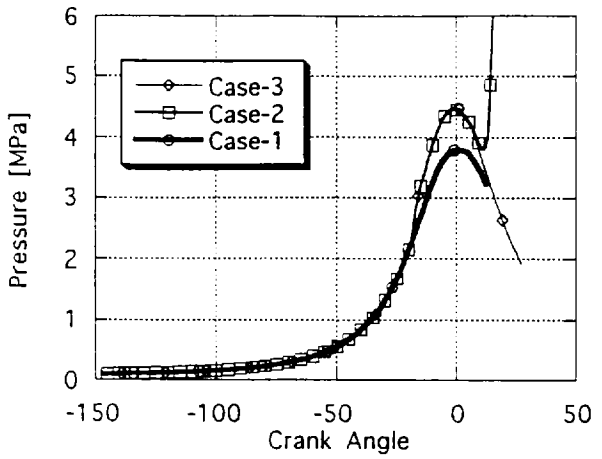

Figure 5 Engine pressure for cases 1,2, and 3.

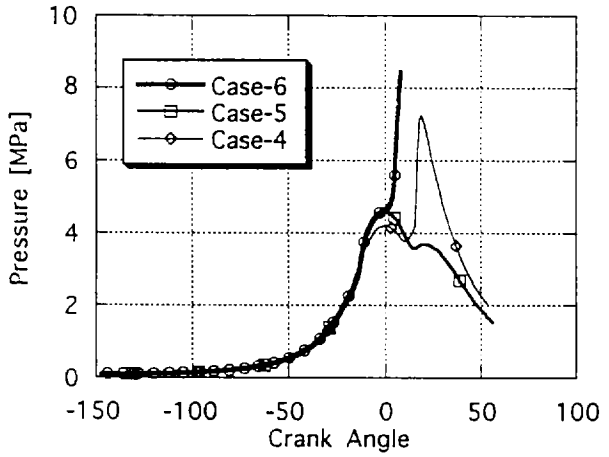

Figure 6 Engine pressure for cases 4, 5, and 6.

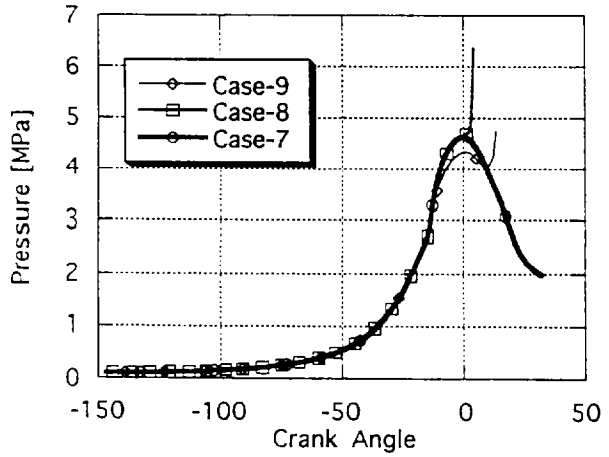

Figure 7 Engine pressure for cases 7, 8, and 9.

The switch from ignition "low-temperature" kinetics model to the combustion "high temperature kinetics model at a particular location occurs when the temperature at that location exceeds 1000 K. Thus the residual fuel did not directly alter the combustion in the engine, but it helped accelerate ignition as is evident in case 2, and is summarized in the last three columns of Table 2 which gives the crank angles at which temperatures of 1000, 1500, and 2000 K are reached in the combustion chamber.

The effect of increasing the duration of injection was significant as seen in the case 3 results in Table 2 as well as in Fig. 5. With the longer injection duration (i.e., lower injection velocities), ignition occurred 10 degrees later and combustion did not develop compared to case 2. This is explained by the poorer atomization that resulted from the lower droplet velocities as they leave the injector nozzle. The lower velocities and the larger droplets both reduce the amount of vaporized fuel.

Reducing the amount of residual fuel to 5% of the total injected fuel amount resulted in partial combustion in case 4 as shown in Fig. 6. Although the onset of ignition was not changed appreciably by using a 5% residual instead of 10% (cases 4 and 2 respectively), the speed and progress of the combustion was significantly reduced in case 4. This demonstrates the importance and impact of a small percentage of the fuel charge that is carried over from one cycle to the following cycle during cold-starting.

The ambient temperature had a significant impact on engine performance. When the ambient air intake temperature was reduced from 273 K to 254 K, ignition was delayed and there was very little combustion, even with the presence of 10% residual fuel as seen in case 5. However, when the composition of the residual fuel was changed to include more cetane which has a higher cetane number, and therefore, a higher tendency to ignite, ignition occurred just before top dead center and combustion started to develop at a rapid pace as seen in case 6 in Fig. 6. This change in engine performance demonstrates the impact of fuel composition on ignition and combustion in the engine.

Finally, the last parameter that was investigated in this study was the engine geometry which has a significant impact on engine performance as seen in Fig. 7. The standard bowl geometry, which is shown in Fig. 4, had a straight-edged bowl. By looking at the spray droplets distribution for the standard straight bowl in Fig 8, it is obvious that the spray impinges on the wall of the piston and slides all the way up until it reaches the cylinder head and then it disperses in all directions parallel to the head. In this case ignition occurs at the stagnation point of the spray near the cylinder head. This is demonstrated in Fig. 8 which shows the temperature contours in the plane of the spray. A high temperature region is seen to exist in the region where the spray impacts the cylinder head. The occurrence of combustion in this region can be explained by the fact that the fuel droplets have sufficient residence time to vaporize there. This result indicates that an engine

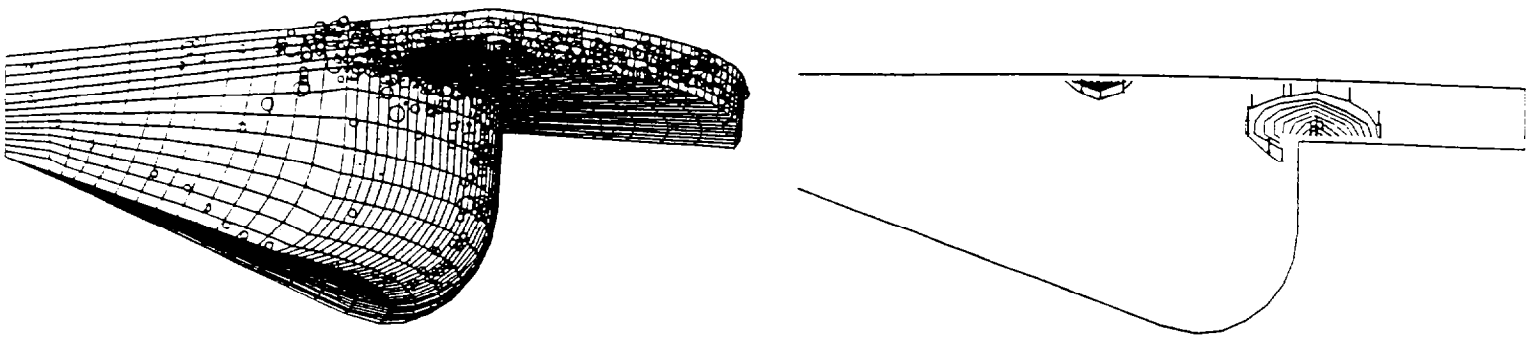

Figure 8 Droplet distribution (at 3° ATDC) and temperature contours near ignition (at 9° ATDC) for Case 4.

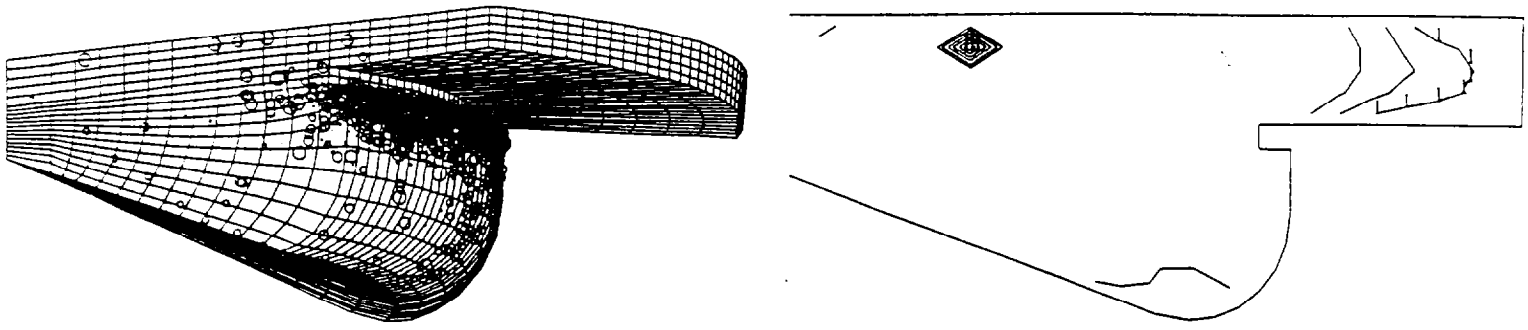

Figure 9 Droplet distribution (at 3° ATDC) and temperature contours near ignition (at 19° ATDC) for Case 7.

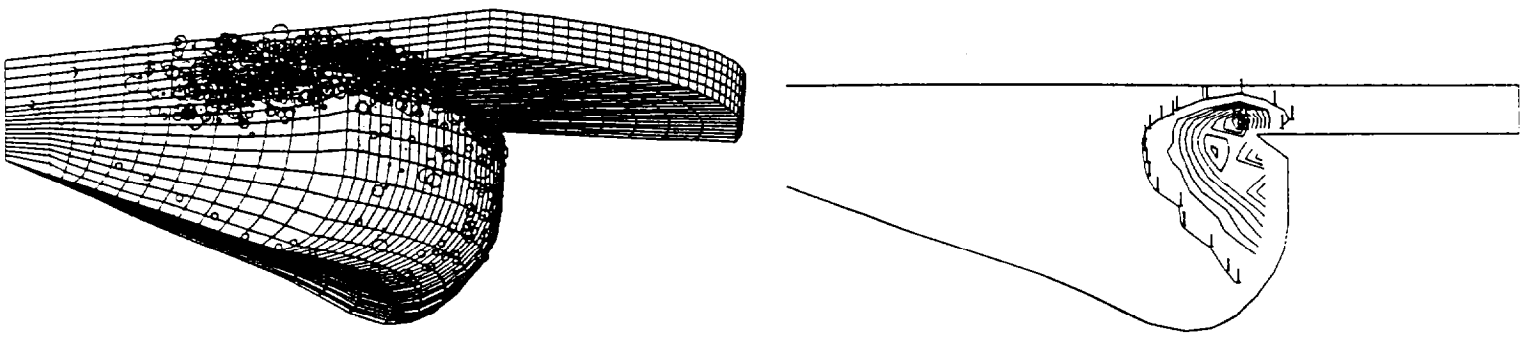

Figure 10 Droplet distribution (at 3° ATDC) and temperature contours near ignition (at 3.1° ATDC) for Case 8.

design that promotes a stagnation region in the fuel spray may exhibit improved cold-starting characteristics.

In an attempt to divert the fuel spray to a warmer region of the engine cylinder gas, a square-edged rim was introduced in the geometry, making the bowl a re-entrant one. However, the fuel droplets were found to accumulate at the lower corner of the rim, and failed to be diverted into the warmer region in the middle of the cylinder, as is evident from Fig. 9. This is also reflected in the engine pressure results for case 7 in Fig. 7, where ignition occurred but due to the poor mixing, combustion was not well-sustained. Finally, a 45° notched rim was introduced in the engine geometry as seen in Fig. 10. In this case, the rim allowed the fuel droplets to impinge on the cylinder head and to be deflected into the warmer regions of the center of the bowl. This is also reflected in Fig. 7 in case 8 where combustion developed right after top dead center at a very fast rate. The same geometry was used with a smaller residual fuel mass (case 9). Ignition started early but the combustion developed at a slower rate.

Another application of an altered engine geometry, is to direct the fuel spray to a specific location on the cylinder head. An ignition aid, such as a glow plug could be placed appropriately in that location to accelerate ignition and sustain combustion under cold starting conditions.

SUMMARY AND CONCLUSIONS

An improved version of the multidimensional computer code, KIVA-II, has been used to study the effects of multicomponent fuel vaporization on diesel engine ignition under cold-starting conditions. Improvements to the code include the implementation of a high pressure multicomponent fuel spray vaporization model that is necessary to model real fuels in a more representative way. The model has been previously tested for single droplets and results were compared favorably to experiments. The model has been also applied to a spray, together with improved atomization and drop breakup models, a drop drag model that accounts for drop distortions, and a spray/wall impingement model with enhanced breakup of impinging drops [4]. In this study the model has been applied to diesel engine computations with a multistep kinetics ignition model that was modified to include fuel (cetane number) effects and a laminar-and-turbulent characteristic-time combustion model, together with a wall heat transfer model that accounts for compressibility, unsteadiness, and a crevice flow model.

The previous spray results indicated the importance of multicomponent fuel drop vaporization at colder ambient temperatures [4]. The present warm engine results show good agreement between measured and predicted cylinder gas pressures for standard conditions. Also the computed engine NOx emission trends were in agreement with expected trends. With these validations in place, the model was used to study the effects of injection timing, intake air temperature, fuel residual, and engine geometry variations under cold-starting conditions.

The predicted cold-starting trends are reasonable and include cases with fully-developed combustion and other cases with border-line ignition. A small amount of vapor fuel residual was shown to enhance ignition and combustion. In addition, the composition of the residual fuel vapor was found to influence ignition significantly. Good atomization of the spray was also shown to shorten the ignition delay. Engine geometry is also an important factor. By appropriate changes in the piston bowl geometry, the fuel spray can be diverted to warmer regions in the engine cylinder to help ignition and to sustain combustion.

Under investigation is the possibility of using split injections, where a small fraction of the fuel is injected early in the compression stroke to help ignition in the same way the fuel residual enhanced ignition.

ACKNOWLEDGMENTS

This work was supported under DOE/NASA-Lewis grant NAG 3-1087 and by the Army Research Office under grant DAAH04-94-G-0328. Support for the computations was provided by Cray Research, Inc., and by the San Diego Supercomputer Center.

REFERENCES

1. Henein, N. A., and Lee, C. S., "Autoignition and Combustion of Fuels in Diesel Engines under Low Ambient Temperatures," SAE paper 861230, 1986.

2. Gonzalez. M.A. , Borman, G.L. and Reitz, R.D., "A Study of Diesel Cold Starting Using Both Cycle Analysis and Multidimensional Computations," SAE Technical Paper 910180, 1991.

3. Lefebvre, A. H., "Atomization and Sprays," Hemisphere Publishing Co., 1989.

4. Ayoub. N. S., and Reitz, R. D., "Multidimensional Computation of Multicomponent Spray Vaporization and Combustion," SAE Technical Paper 950285, 1995.

5. Amsden, A.A., O'Rourke, P.J. and Butler, T.D., "KIVA-II - A Computer Program for Chemically Reactive Flows with Sprays," Los Alamos National Labs., LA-11560-MS, 1989.

6. Kong, S.C. and Reitz, R.D., "Spray Combustion Processes in Internal Combustion Engines," in

Recent Advances in Spray Combustion, AIAA Series, Editor K.K. Kuo, to appear 1995.

7. Reitz, R.D. "Assessment of Wall Heat Transfer Models for Premixed-Charge Engine Combustion Computations," SAE Technical Paper 910267, 1991.

8. Reitz, R.D. and Kuo, T.W. "Modeling of HC Emissions due to Crevice Flows in Premixed-Charge Engines," SAE Technical Paper 892085, 1989.

9. Jin, J. D., and Borman, G. L., "A Model for Multi-component Droplet Vaporization at High Ambient Pressures," SAE Technical paper 850264, 1985.

10. Prausnitz, J. M., "Molecular Thermodynamics of Fluid-Phase Equilibria," Prentice-Hall, NJ, 1969.

11. Reid, R. C., Prausnitz, J. M., and Sherwood, T. K., "The Properties of Gases and Liquids," Third Edition, McGraw-Hill, New York, 1977.

12. El-Wakil, M. M., Priem, R. J., Brikowski, H. J., Meyers, P. S., and Uyehara, O. A., "Experimental and Calculated Temperature and Mass Histories of Vaporizing Drops," NACA TN 3490, 1956.

13. Abramazon, B., and Sirignano, W. A., "Approximate Theory of a Single Droplet Vaporization in a Convective Field," *ASME/JSME Thermal Engineering Conference*, Vol. 1, pp. 11-18, 1987.

14. Prausnitz, J. M., Chuen, P. L., "Computer Calculations for High-Pressure Vapor-Liquid Equilibria," Prentice-Hall, NJ, 1968.

15. Halstead, M., Kirsh, L. and Quinn, C. "The Autoignition of Hydrocarbon Fuels at High Temperatures and Pressures - Fitting of a Mathematical Model," *Combust. Flame*, 30, 45-60, 1977.

16. Kong, S.C. and Reitz, R.D. "Multidimensional Modeling of Diesel Ignition and Combustion Using a Multistep Kinetics Model," ASME Transactions, *Journal of Engineering for Gas Turbines and Power*, Vol. 115, pp. 781-789, 1993.

17. Kong, S.C., Han, Z., and Reitz, R.D., "The Development and Application of a Diesel Ignition and Combustion Model for Multidimensional Engine Simulations," SAE Paper 950278, 1995.

18. Ramos, J.I., Internal Comustion Engine Modeling, Hemisphere Publishing, NY, 1989.

19. Heywood, J.B., Internal Combustion Engine Fundamentals, McGraw-Hill, NY, 1988.

20. Bergeron, C.A. and Hallett, W.L.H. "Ignition Characteristics of Liquid Hydrocarbon Fuels as Single Droplets," *Canadian J. of Chem. Engng*, 67, 142-149, 1989.

21. Kong, S.C., Ayoub, N. and Reitz, R.D. "Modeling Combustion in Compression Ignition Homogeneous Charge Engines," SAE Technical Paper 920512, 1992.

22. Magnussen, B. F., and Hjertager, B. H., "On Mathematical Modeling of Turbulent Combustion with Special Emphasis on Soot Formation and Combustion," *16th Symposium (International) on Combustion*, Combustion Institute, pp. 719-729, 1976.

23. Ayoub, N. S., and Reitz, R. D., "Multidimensional Computation of Multicomponent Fuel Spray Vaporization," Central States Section of the Combustion Institute Technical Meeting Proceedings, pp. 147-152, 1994.

24. Patterson, M. A., Kong, S. K., Hampson, G. J., and Reitz, R. D., "Modeling the Effects of Fuel Injection Characteristics on Diesel Engine Soot and NOx Emissions," SAE paper 940523, 1994.

25. Nehmer, D.A., "Measurement of the Effect of Injection Rate and Split Injections on Diesel Engine Soot and NOx Emissions," MS Thesis, Univ. of Wisconsin, 1993.

26. Tow, T., Pierpont, A. and Reitz, R.D. "Reducing Particulates and NOx Emissions by Using Multiple Injections in a Heavy Duty D.I. Diesel Engine," SAE Paper 940897, 1994.

27. Giangregorio, R.P., Zhu, Y. and Reitz, R.D., "Application of Schlieren Optical Techniques for the Measurement of Gas Temperature and Turbulent Diffusivity in a Diesel Engine," SAE Technical Paper 930869, 1993.

28. Sweetland, P. and Reitz, R.D., "Particle Image Velocimetry Measurements in the Piston Bowl of a DI Diesel Engine," SAE Paper 940283, 1994.

29. Rutland, C.J., Pieper, C. and Hessel, R., "Intake and Cylinder Flow Modeling with a Dual-Valve Port," SAE Technical Paper 930069, 1993.

30. Nehmer, D.A. and Reitz, R.D., "Measurement of the Effect of Injection Rate and Split Injections on Diesel Engine Soot and NOx Emissions," SAE Paper 940668, 1994.

31. Tree, D., "Soot Particle Size and Number Density Measurements in a Direct Injection Diesel Engine Using Light Scattering, Radiation, and Extinction," Ph.D. Thesis, Univ. of Wisconsin, 1992.

32. Gonzalez, M.A., Lian, Z.W. and Reitz, R.D. "Modeling Diesel Engine Spray Vaporization and Combustion," SAE Technical Paper 920579, 1992.

33. Poublon, M., Patterson, D., and Boerma, M., "Instantaneous crank speed variations as related to engine starting," SAE Paper 850482, 1985.

34. Henein, N. A., and Zadeh, A., "Diesel cold starting: Actual cycle analysis under borderline conditions," SAE Paper 900441, 1990.